Frontiers in Bioscience Landmark

Front. Biosci. (Landmark Ed). **2022**; 27(1): 008
http://doi.org/10.31083/j.fbl2701008

Original Research

In vivo and *in vitro* neuroprotective effects of maca polysaccharide

Yi Zhou[1,2,†], Lemei Zhu[1,2,†], Haigang Li[1,2], Wenqing Xie[3], Juan Liu[1,2], Yuan Zhang[1,2], Yusheng Li[3,*], Chenggong Wang[3,*]

[1]Hunan Key Laboratory of the Research and Development of Novel Pharmaceutical Preparations, 410219 Changsha, Hunan, China
[2]Academician Workstation, Changsha Medical University, 410219 Changsha, Hunan, China
[3]Department of Orthopedics, Xiangya Hospital Central South University, 410008 Changsha, Hunan, China
*Correspondence: liyusheng@csu.edu.cn (Yusheng Li); wangchenggong@csu.edu.cn (Chenggong Wang)
[†]These authors contributed equally.

Academic Editor: Marcello Iriti
Submitted: 10 August 2021 Revised: 20 November 2021 Accepted: 8 December 2021 Published: 6 January 2022

Abstract

Objective: To explore the protective effect of MP on oxidative damage *in vivo* and *in vitro*. **Methods**: A mouse aging model was induced by intraperitoneal injection of D-galactose (D-gal), and pathological changes in the hippocampal ultrastructure were observed by transmission electron microscopy. The activity of glutathione peroxidase (GSH-Px) and the levels of malondialdehyde (MDA) in brain tissues were evaluated with GSH-Px and MDA assay kits. An MTT assay was used to detect the viability of the model SH-SY5Y cells with H_2O_2-induced damage, and a lactate dehydrogenase (LDH) kit was used to evaluate LDH leakage. Reactive oxygen species (ROS) levels and cell cycle arrest were analyzed by flow cytometry, and cleaved caspase 3 and P53 protein expression was determined by western blot analysis. **Results**: Demonstrated that MP increased GSH-Px activity, reduced MDA levels, and attenuated the cell damage induced by H_2O_2. Furthermore, MP protected neuronal cells from oxidative stress through a mechanism including a decrease in LDH leakage and reversal of H_2O_2-induced cell morphological damage. MP treatment alleviated the H_2O_2-induced increases in ROS levels, inhibited apoptosis, relieved cell cycle arrest, and downregulated cleaved caspase 3 and P53 protein expression. **Conclusions**: MP is a novel antioxidant with neuroprotective effects.

Keywords: Neuroprotective effect; MP; Reactive oxygen species; D-galactose; SH-SY5Y cells

1. Introduction

The plant *Lepidium meyenii* Walp. (maca) originated in the Andes where the temperature is low at high altitudes between 3700 and 4450 m, and it has traditionally been used to enhance fertility [1,2]. The major active ingredients in maca are polysaccharides, macamides, macaenes, and alkaloids [3]. In 2011, the Chinese government classified maca as a functional food, and this plant is well-known for being nutrient-rich and for promoting fertility in humans [4]. In many studies, maca has been shown to scavenge free radicals and protect cells against oxidative stress [3]. Oxidation can produce energy to promote essential biological processes in many organisms. However, reactive oxygen species (ROS) are often overproduced during oxidation, resulting in an imbalance in the antioxidant defense system [5]. Furthermore, excessive oxidative stress plays a vital role in the aging process [6,7]. Maca is a source of macamides and polysaccharides, which can combat oxidative stress and damage in human erythrocytes [8]. In addition, previous studies have indicated that maca polysaccharide (MP) effectively scavenges 1,1-Diphenyl-2-picrylhydrazyl (DPPH) and peroxyl radicals to protect erythrocytes against H_2O_2-induced hemolysis by inhibiting the generation of malondialdehyde (MDA) [9].

D-Galactose (D-gal) is commonly used to establish aging models because it can induce oxidative damage [10–12]. Small amounts of D-gal can be metabolized and utilized [13]. However, exogenous supplementation with excessive D-gal causes large amounts of D-gal to accumulate; the resulting high D-gal levels alter oxidase activity and lead to the production of large amounts of oxidation products, which further affect physiological structure and function [14].

ROS, which include oxygen ions, peroxides, and oxygen-containing free radicals, are potentially dangerous byproducts of normal aerobic cellular metabolism in organisms [15,16]. Increasing evidence has shown that excessive ROS levels during neuronal cell apoptosis are related to various chronic neurodegenerative disorders [17], as neuronal cells are thought to be more sensitive to oxidative stress than cells in other tissues [18]. Exogenous supplementary antioxidants may protect cells from the damaging effects of ROS by scavenging free radicals [19,20]. Increasing attention has been given to identifying effective and safe natural antioxidants due to the carcinogenicity of synthetic antioxidants. Polysaccharides are widely distributed in various organisms, and polysaccharides isolated from many kinds of plants have been shown to exhibit strong antioxidant ac-

tivity against free radicals [21,22]. Thus, these compounds should be further investigated as potential novel antioxidants.

In the present study, MP was extracted from maca. As SH-SY5Y cells are sensitive to the apoptosis- and cytotoxicity-inducing effects of H_2O_2 [23], the effects of MP on H_2O_2-treated human neuronal SH-SY5Y cells were evaluated *in vitro*. For *in vivo* experiments, model mice with D-gal-induced oxidative stress-related aging were administered MP, and the effects of MP on brain tissue were observed. This study aimed to provide a theoretical basis for further research on MP as a medicine and to provide a material basis for further research on maca.

2. Materials and methods

2.1 Reagents and materials

Maca was purchased from Lijiang Green Hanson Biotechnology Development Co., Ltd. (Lijiang, China). Dulbecco's modified Eagle's medium/Ham's nutrient mixture F-12 (DMEM/F-12, 1:1) was purchased from HyClone Laboratories (Logan, UT, USA). The human neuroblastoma cell line SH-SY5Y was obtained from the Cell Bank of the Type Culture Collection of the Chinese Academy of Sciences (Shanghai, China), while 3-(4,5-dimethylthiazol-2-yl)-2,5-diphenyltetrazolium bromide (MTT), trypsin-EDTA, fetal bovine serum (FBS), penicillin and streptomycin were purchased from Gibco-BRL (Grand Island, NY, USA). Radioimmunoprecipitation assay (RIPA) buffer was purchased from Shanghai Wellfeng Biotech Co., Ltd. (Shanghai, China). A propidium iodide (PI)/RNase staining buffer kit was purchased from Becton Dickinson and Company (Franklin Lakes, NJ, USA), and an Annexin V Cell Apoptosis Analysis Kit and 2,7-dichlorofluorescein diacetate (DCFH-DA) were purchased from Sungene Biotech Co., Ltd. (Tianjin, China). D-Gal was obtained from Life Sciences. A bicinchoninic acid (BCA) protein concentration determination kit, GSH-Px assay kit, MDA assay kit, and LDH assay kit were obtained from Nanjing Jiancheng Bioengineering Institute (Nanjing, China). Rabbit anti-caspase 3 (#8231) and rabbit anti-cleaved caspase 3 (# 8231) antibodies were obtained from Cell Signaling, and anti-P53 (mouse monoclonal, AP062), anti-tubulin (mouse monoclonal, AT819), HRP-labeled goat anti-mouse and rabbit IgG (H + L) (A0412) antibodies were obtained from Beyotime Biotechnology (Shanghai, China). All other chemicals were of analytical grade and were obtained from Nanjing Jiancheng Bioengineering Institute (Nanjing, China).

2.2 Identification of maca

The content of N-benzyl-hexadecanamide in maca was determined by SPD-M20A high-performance liquid chromatography (Shimadzu, Japan). N-Benzyl-hexadecanamide (20 mg; China Food and Drug Administration) was used as a reference substance, and 5 mg was weighed into a 20 mL volumetric flask, shaken and completely dissolved as a reference substance stock solution. An Accucore™ C18 column (particle size 5.0 μm; size 4.6 $\times$ 250 mm; Thermo Fisher Scientific, Inc. (Shanghai, China) was used, and the mobile phase solvents included mobile phase A (0.005% trifluoroacetic acid in water) and mobile phase B (0.005% trifluoroacetic acid in acetonitrile). The gradient conditions were as follows: 0–35 min, 55–95% phase B; 35–40 min, 95–100% phase B; flow rate, 1.0 mL/min. The injection volume was 20 μL, the column temperature was 30 °C, and the detection wavelength was 210 nm [24].

2.3 MP extraction

A dried maca block was crushed, and the powder was extracted twice with distilled water (1:20, w:v) at 95 °C for 2 h each time. The solutions were combined and filtered, centrifuged, concentrated, and adjusted to pH 6.5 with phosphate buffer. Two milliliters were incubated in a 60 °C water bath for 3 h after thorough mixing. Then, 1 mL of amylase was added, and the mixture was incubated for another 2 h. After enzymatic hydrolysis, the solution was placed in a boiling water bath for 10 min to inactivate the enzyme, cooled to room temperature and centrifuged; the supernatant was then deproteinized using the Sevage method [25]. Subsequently, the deproteinized supernatant was added to 95% ethanol at a ratio of 1:5 and vigorously stirred, and the mixture was placed at 4 °C overnight. After centrifugation, the precipitate was washed successively with absolute ethanol, acetone and ether and then vacuum-dried at 40 °C to obtain the crude MP. The carbohydrate content in the MP was determined by the phenol-sulfuric acid method [26].

2.4 Effects of MP on D-gal-induced brain impairment in mice

2.4.1 Animals

Healthy ICR male mice (8 weeks, 29–32 g, SPF grade) were purchased from Hunan Slake Jingda Experimental Animal Co., Ltd. (certificate number: SCXK (XIANG) 2019-0004). The mice were allowed to adapt for 7 days in an environment with an ambient temperature of 19–21 °C and a relative humidity of 50–60% under a 12 h/12 h light/dark period, and all mice were allowed to eat and drink freely.

2.4.2 Animal models

Fifty ICR mice were randomly divided into 5 groups (10 mice in each group). The mice in group 1, which served as the control group, received saline (0.9% NaCl) daily by intraperitoneal (i.p.) injection and received distilled water without MP orally. The mice in groups 2–5 received 500 mg/kg D-gal daily by i.p. injection for eight weeks [27]. The D-gal-treated mice in group 2, which served as the D-gal group, also received distilled water without MP. The

mice in groups 3–5 received 75, 150 or 300 mg/kg MP in distilled water orally for eight weeks. After 8 weeks, the animals were sacrificed, and brain tissue samples were collected. Mouse hippocampal dentate gyrus samples from the first three mice in each group were used for transmission electron microscopy (TEM) analysis, and the brain cortices of each group of mice were used to detect GSH-Px activity and MDA content.

2.5 Determination of activity and MDA content in mouse brain tissue

Brain cortex samples were obtained from each group. Subsequently, 100 mg of cortex tissue from each mouse was placed in a glass homogenization tube, after which 1 mL phosphate buffered solution (PBS) was added, and the sample was homogenized on ice for 10 min to produce a 10% brain tissue homogenate. Finally, the appropriate kit was used to perform the test according to the instructions. MDA content was measured by the thiobarbituric acid reactive substance (TBARS) method [28]. Briefly, the homogenate was mixed with 3 mL of H_3PO_4 solution (1%, v/v), after which 1 mL of thiobarbituric acid solution (0.67%, w/v) was added. The mixture was incubated at 95 °C in a water bath for 45 min. The colored complex was extracted into N-butanol, and the absorption at 532 nm was measured using tetramethoxypropane as a standard. MDA levels are expressed as nmol/mg protein. GSH-Px activity was determined by quantifying the catalyzed reaction rate of H_2O_2 and GSH [29]. The enzymatic reaction in tube containing nicotinamide-adenine dinucleotide phosphate (NADPH), reduced GSH, sodium azide and glutathione reductase was initiated by the addition of H_2O_2. The change in absorbance at 340 nm was monitored. GSH-Px activity is expressed as U/mg protein.

2.6 TEM analysis

The mouse hippocampal dentate gyrus samples were fixed in a 4% paraformaldehyde solution (4 °C) and then moved to 1% osmium tetroxide, after which ethanol and acetone were used for gradual dehydration. Then, the samples were embedded in epoxy resin 618, sliced into ultrathin sections, double-stained with uranyl acetate and citric acid, and finally observed and imaged with a transmission electron microscope (Hitachi 7100, Hitachi, Ltd., Tokyo, Japan).

2.7 Effects of MP on H_2O_2-induced oxidative impairment in SH-SY5Y cells

2.7.1 Cell culture and treatment

Cells were cultured in 25 cm^2 flasks in DMEM/F-12 (DMEM:F12 = 1:1) supplemented with 10% (v/v) FBS, 100 U/mL penicillin, and 100 μg/mL streptomycin at 37 °C under 5% CO_2 in an incubator [30]. The cell culture medium was replaced every three days. Once the cells reached 80–90% confluence, they were subcultured. SH-SY5Y cells were seeded in well plates at a density of 8×10^4 cells/mL and cultured for 24 h.

2.7.2 Measurement of cell viability

Cells were cultured in 96-well plates at a density of 8×10^4 cells/mL in a volume of 150 μL per well for 24 h before treatment. The cells were cultured in different concentrations of H_2O_2 (100–800 μM) for 6 h, and then an MTT reduction assay was used to evaluate the effects of the different concentrations of H_2O_2 on the viability of the SH-SY5Y cells. The appropriate concentration of H_2O_2 was determined for modeling (cell survival rate 50–60%).

Other cells were cultured in 96-well plates at a density of 8×10^4 cells/mL in a volume of 150 μL per well for 24 h before treatment. The SH-SY5Y cells were pretreated with various concentrations of MP (25, 50 and 100 μg/mL) for 24 h and then exposed to 300 μM H_2O_2 for 6 h. Subsequently, 15 μL of MTT (5 mg/mL in PBS) was added to each well, and the cells were incubated at 37 °C for 4 h. Then, the supernatant was carefully aspirated, 150 μL of dimethyl sulfoxide (DMSO) was added to each well to dissolve the precipitate, and the absorbance was measured at 490 nm with a microplate reader [31–33]. Cell viability is expressed as the percentage of control cells.

2.8 Measurement of LDH activity

Cells were cultured in 6-well plates at a density of 8×10^4 cells/mL in a volume of 2 mL per well for 24 h before treatment. Then, the cells were incubated with MP for 24 h, 300 μM H_2O_2 was added to the culture medium, and the cells were cultured for another 6 h. After the cells were treated as described previously, the cell morphology was observed, and images were obtained under an inverted microscope (Olympus CKX53). The cell supernatant was collected, and a kit was used to measure LDH activity according to the manufacturer's instructions.

2.9 Flow cytometry detection of apoptotic cells

A commercial Annexin V-FITC detection kit was used to observe the effect of MP on H_2O_2-induced apoptosis. In accordance with the manufacturer's instructions, cells in a 6-well plate that had been treated as described previously were digested with 0.25% trypsin, collected and processed into a single-cell suspension. The cells were then stained following the manufacturer's protocols. Flow cytometry was performed on a Beckton Dickinson FACScan (Franklin Lakes, NJ, USA) and analyzed using CellQuest Pro software (version 3.3, Beckton Dickinson).

2.10 Determination of intracellular ROS levels

The oxidation-sensitive fluorescent probe DCFH-DA was used to evaluate the generation of ROS. Cells in six-well plates were used after being treated as described previously. Briefly, the cells were incubated with DCFH-DA (final concentration 10 μmol/L) in the dark at 37 °C for 30

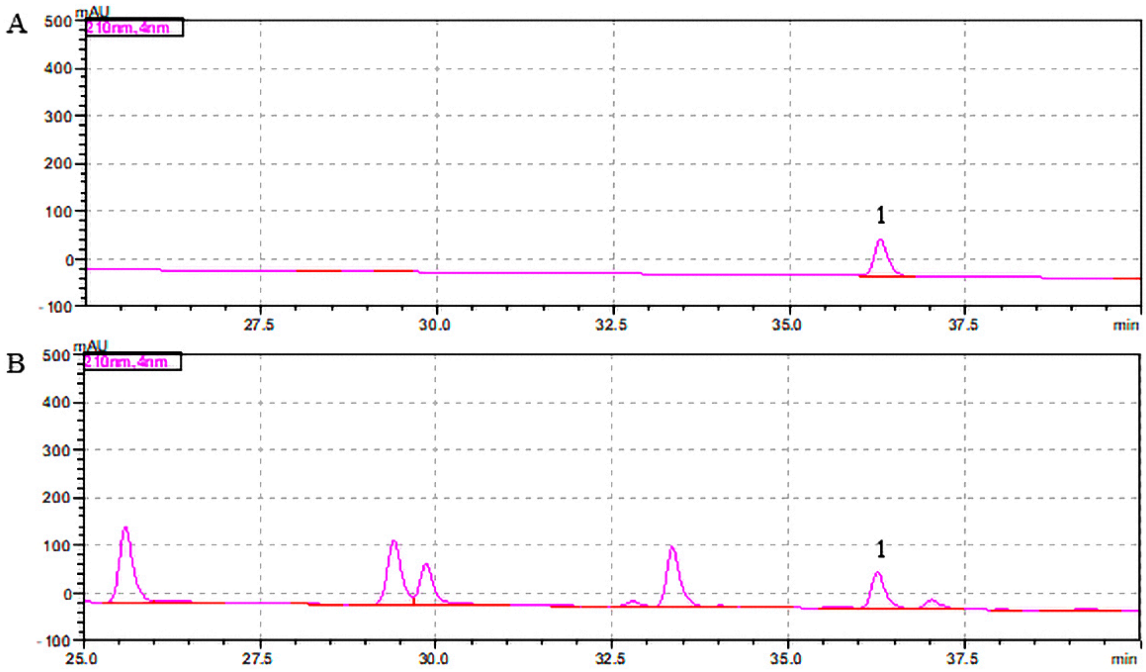

Fig. 1. Maca extract chromatogram. (A) Standard. (B) Maca extract. The number 1 indicates N-benzyl-hexadecanamide.

min, and then the relative fluorescence intensity was measured using an excitation wavelength of 485 nm. The cells loaded with DCFH-DA were examined by flow cytometry. The measured fluorescence value is expressed as a percentage of the fluorescence of the control cells.

2.11 Determination of cell cycle status

A PI/RNase staining buffer kit was used to assess the effects of MP on H_2O_2-induced changes in the cell cycle. Cells in 6-well plates were collected after being treated as described previously. The pellets were then resuspended in ice-cold 70% ethanol and fixed at 4 °C for 24 h. Then, the cells were washed and resuspended in 0.5 mL of PI/RNase staining solution. The cells were stained at room temperature in darkness for 30 min. The percentages of cells in the G0/G1, S, and G2/M phases of the cell cycle were determined by flow cytometry, and the data were analyzed by utilizing Mod FitLT software (BD), version 2.0 (Software House, USA).

2.12 Western blot assay of signaling proteins

The expression levels of P53, caspase 3 and cleaved caspase 3 in SH-SY5Y cells were examined by western blot analysis. After being treated as described previously, cells were trypsinized and collected. Then, the pelleted cells were lysed in 100 μL of RIPA buffer on ice for 15 min, after which the lysates were centrifuged at 12,000$\times$ g for 10 min at 4 °C. Subsequently, the supernatants were collected, and the protein concentrations were determined with a BCA protein assay kit. After boiling the samples in loading buffer for 5 min, the proteins were separated by 12% sodium dodecyl sulfate–polyacrylamide gel electrophoresis (SDS–PAGE) at 100 V for 60 min and then transferred to nitrocellulose membranes using a transfer apparatus for 50 min at 300 mA. Then, the membranes were rinsed in PBST (PBS with 0.1% Tween 20), blocked with 5% nonfat dry milk in PBST at room temperature for 60 min and probed with the following primary antibodies on a platform shaker overnight at 4 °C: mouse anti-P53 mAb (1:1000), rabbit anti-caspase 3 (8G10) mAb (1:1000), rabbit anti-cleaved caspase 3 mAb (1:1000) and mouse anti-tubulin mAb (1:1000). The membranes were washed six times for 5 min each using PBST. After that, the cells were incubated with the appropriate HRP-conjugated secondary antibody at room temperature for another 1 h and washed again six times in PBST buffer. The membranes were then incubated with enhanced chemiluminescence (ECL) substrate solution (Thermo Scientific, Waltham, MA, USA) for 5 min according to the manufacturer's instructions and visualized with radiography film.

2.13 Statistical analysis

The results are reported as the mean $\pm$ SD. Statistical evaluation was performed with Student's *t*-test when two groups were compared, and $p < 0.01$ or $p < 0.05$ was considered to indicate a significant difference.

3. Results

3.1 Phytochemical analysis of maca

High Performance Liquid Chromatography (HPLC) analysis of the maca composition revealed the presence of N-benzyl-hexadecanamide (retention time [t_R] = 36.37 min, peak 1; Fig. 1) at a concentration of 0.077%.

Table 1. Effects of MP on the activity of related enzymes in mouse brain tissue ($\bar{x} \pm s$, n = 10).

Group	GSH-Px (U/mg protein)	MDA (nmol/mg protein)
Control	727 ± 83	0.9 ± 0.11
D-gal	492 ± 58$^{\#\#}$	1.6 ± 0.15$^{\#\#}$
D-gal + MP (75 mg/kg)	573 ± 71*	1.1 ± 0.09**
D-gal + MP (150 mg/kg)	610 ± 49**	1.2 ± 0.12**
D-gal + MP (300 mg/kg)	652 ± 28**	1.1 ± 0.13**
F	16.27	35.14
p	<0.01	<0.01

Note: Compared with the control group, $^{\#\#}p < 0.01$; compared with the D-gal group, $^{**}p < 0.01$, $^{*}p < 0.05$.

3.2 Extraction of polysaccharides from maca

Using the formula polysaccharide yield (%) = polysaccharide weight in the extract (g)/weight of maca (g), the yield of MP was calculated to be 13.36%. The purity of carbohydrates in MP was determined by the phenol-sulfuric acid method to be 71.54%.

3.3 Effect of MP on GSH-Px activity and MDA content in mouse brain tissue

The GSH-Px enzyme activity in brain tissue was significantly different among the groups of mice (F = 16.27, $p < 0.01$). In the presence of D-gal, the GSH-Px enzyme activity of the D-gal group was 492 ± 58 U/mg protein, while that of the control group was significantly higher at 727 ± 83 U/mg protein ($p < 0.01$). Compared to that in the D-gal group, the enzyme activity in the low-, medium- and high-MP groups was significantly higher ($p < 0.05$ or $p < 0.01$). The MDA content in brain tissue also significantly differed among the groups ($F = 35.24, p < 0.01$). There was a significant difference in MDA content between the D-gal and control groups, and in all MP administration groups, the MDA content was significantly lower than that of the D-gal group ($p < 0.01$, Table 1).

3.4 Effects of MP on the brain cortex ultrastructure in D-gal-treated model mice

Pathological changes in the brain cortex ultrastructure in mice were observed by electron microscopy. The control mice showed clear structures; large, round nuclei; complete, smooth nuclear membranes; uniform chromatin distributions; and abundant cytoplasm (Fig. 2A). In contrast, the D-gal group exhibited pyknosis, an incomplete nuclear membrane structure, cracks in the perinucleus, aggregated nuclear chromatin, and an expanded cytoplasmic endoplasmic reticulum (Fig. 2B). The cell structure in the low-, medium- and high-MP groups tended to be normal, with large, round nuclei; a complete nuclear membrane structure; and a uniform chromatin distribution (Fig. 2C–E).

3.5 Protective effect of MP against H_2O_2-induced SH-SY5Y cell injury

SH-SY5Y cells were cultured with H_2O_2 (100-800 μM) for 6 h, and cell viability was detected by MTT assay. The results showed that all assayed concentrations induced significant decreases in cell survival in a dose-dependent manner ($p < 0.01$). In the presence of 300 μM H_2O_2, cells exhibited only 53.0 ± 4.58% (mean ± SD, n = 8) of the viability of control cells (Fig. 3A). Therefore, 300 μM H_2O_2 treatment for 6 h was used to induce SH-SY5Y cell injury in the following experiments. As shown in Fig. 3B, the cell viabilities were compared among the groups, and significant differences from the viability of the H_2O_2 group were observed ($F = 93.39, p < 0.01$). Specifically, cell viability was significantly increased in the low-, medium- and high-MP groups ($p < 0.05$ or $p < 0.01$). The effects of MP were also confirmed through morphological observations (Fig. 3C). LDH activity was found to differ significantly among the groups (F = 1350, $p < 0.01$). As shown in Fig. 3D, a significant increase in LDH leakage was observed after 6 h of exposure to 300 μM H_2O_2, indicating an increase in cell toxicity, while MP treatment significantly attenuated this increase in LDH outflow ($p < 0.01$).

3.6 Protective effect of MP on SH-SY5Y cells against H_2O_2-induced apoptosis

The percentage of apoptotic cells was measured by flow cytometry using double Annexin V and PI staining. The apoptosis rate significantly different among groups (F = 219.6, $p < 0.01$). As shown in Fig. 4, 6.9 ± 0.78% of cells were apoptotic in the control group. After 300 μM H_2O_2 treatment, the percentage of positive cells increased to 34.63 ± 1.34%, significantly higher than the value in the control group ($p < 0.01$). However, this increase was significantly attenuated by pretreatment with 50 and 100 μg/mL MP ($p < 0.01$; Fig. 4A,B).

3.7 MP inhibits the H_2O_2-induced generation of ROS

The levels of intracellular ROS generated after H_2O_2 treatment were quantified by DCFH-DA fluorescence analysis and found to differ significantly among groups (F =

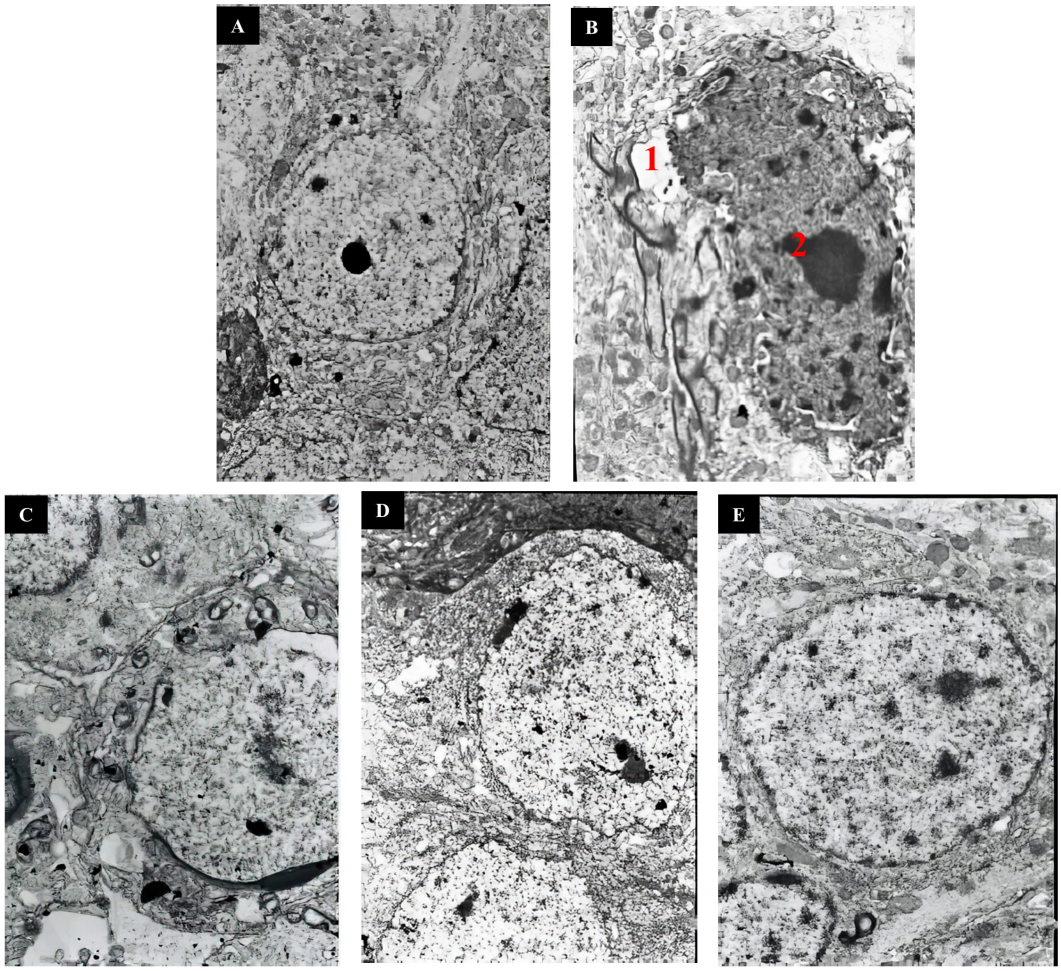

Fig. 2. Ultrastructural pathology of mouse brain slides. (A) Control group. (B) D-gal group. (C) D-gal + MP (75 mg/kg) group. (D) D-gal + MP (150 mg/kg) group. (E) D-gal + MP (300 mg/kg) group. Original magnification: 4000× (A), 4500× (B), 4500× (C), 3500× (D), and 4500× (E). Notes: 1: incomplete nuclear membrane structure, 2: aggregated nuclear chromatin.

85.69, $p < 0.01$). The cells incubated with 300 μM H_2O_2 showed significantly higher intracellular ROS levels than the untreated cells. As shown in Fig. 4C, cells pretreated with MP (100 μg/mL) showed significantly lower intracellular ROS levels than H_2O_2-treated cells without pretreatment ($p < 0.01$), indicating that MP was able to block (attenuate) the production of (and/or scavenge) ROS.

3.8 MP relieves H_2O_2-induced cell cycle arrest

The periodic distribution of cells in the G1, S, and G2/M phases was found to differ significantly among groups ($F = 75.01$, $p < 0.01$; $F = 48.1$, $p < 0.01$; $F = 1.675$, $p < 0.01$). Compared to that in the control group (36.1%), the percentage of S-phase cells in the H_2O_2 group was significantly higher (75.43%), while those in the low-, medium- and high-MP groups were not as high at 70.93%, 67.95%, and 46.46%, respectively; however, the percentage in the high-dose group was significantly elevated ($p < 0.01$). Therefore, a specific concentration of MP was able to alleviate the S-phase cell cycle arrest caused by H_2O_2 (Fig. 4D). The influence of MP on the distribution of cells in other cycle phases was likely related to the effects on cell cycle arrest in the S phase.

3.9 Effect of MP on related protein expression

We investigated the ability of MP to modulate the activation of two signaling proteins. The results showed that SH-SY5Y cells treated with 300 μM H_2O_2 exhibited significant increases in the levels of P53 and cleaved caspase 3, while cells pretreated with MP (50, 100 μg/mL) showed significantly reduced expression of these two proteins ($p < 0.01$) (Fig. 5).

4. Discussion

N-Benzyl-hexadecanamide is a relatively abundant macamide component in maca, and chromatography showed that the N-benzyl-hexadecanamide content in the present study was similar to that described in previous studies [34]. Research on neurological diseases has shown that oxidative stress is associated with neurological dete-

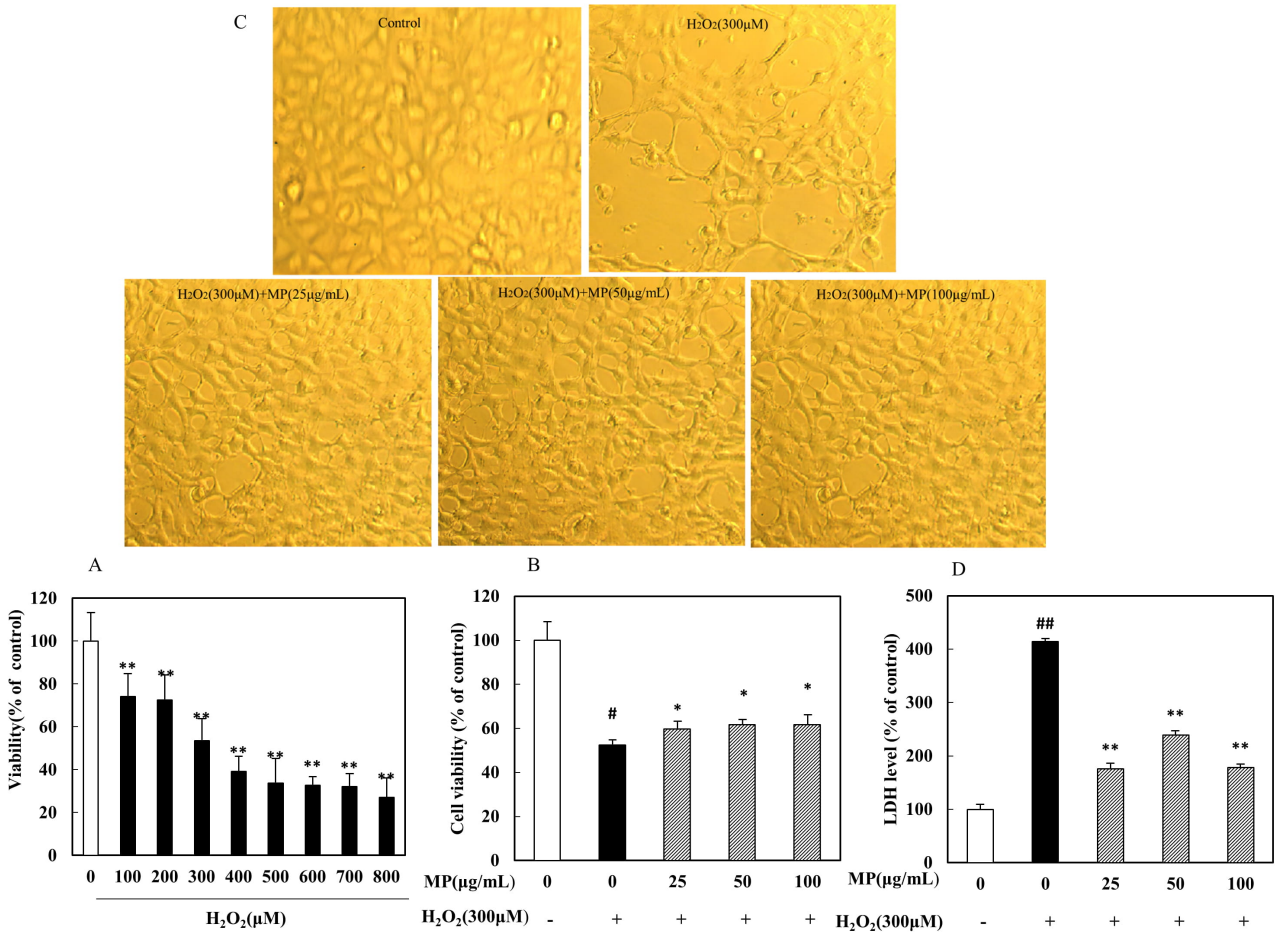

Fig. 3. Protective effect of MP against H_2O_2-induced SH-SY5Y cell injury (n = 8). (A) Dose-dependent toxic effects of different H_2O_2 concentrations on cells. (B) Viability of SH-SY5Y cells. (C) Morphological alterations in SH-SY5Y cells. (D) Release of LDH. All data are presented as the means ± SDs from three independent experiments performed in triplicate. Note: $^{\#\#}p < 0.01$ versus the control group; $^{*}p < 0.05$, $^{**}p < 0.01$ versus the H_2O_2 group.

rioration in many neurodegenerative disorders, including Alzheimer's disease and Parkinson's disease [35]. Therefore, removing excess ROS, inhibiting ROS production and preventing cell death induced by excessive oxidative stress are effective means of protecting the nervous system. In recent years, great efforts have been made to find safer and more efficient natural antioxidants with neuroprotective potential. Polysaccharides, which are major bioactive components in various plants, have received increasing attention due to their antiviral, anticancer, anti-inflammatory, and antioxidant activities and their neuroprotective effects [36].

In organisms, ROS with unpaired electrons and other ROS can be removed by GSH-Px and other enzyme systems. The level of MDA, a lipid peroxide formed by oxidative stress, directly reflects the degree of oxidation in the body [37]. In the present study, MP significantly increased GSH-Px activity and reduced MDA levels. According to the TEM results, the aggregation of neuronal chromatin in the hippocampal dentate gyrus was significantly alleviated in the MP administration group compared with the D-gal group, and the cell structure tended to be normal in the MP group. Therefore, MP effectively alleviated D-gal-induced oxidative stress in mice.

H_2O_2 is a commonly used oxidative stress inducer [38]. We sought to determine the protective effect of MP against H_2O_2-induced injury in SH-SY5Y cells, as H_2O_2 causes apoptosis in SH-SY5Y cells through oxidative stress. We confirmed that treating cells with H_2O_2 resulted in a dose-dependent loss of cell viability. Pretreatment with different concentrations of MP greatly increased cell viability, which was further confirmed by morphological observations and an LDH release assay. LDH is present in all cells in the human body, and when cells are injured by H_2O_2, it is quickly released into the cell culture medium [39]. Thus, stronger LDH activity in the culture supernatant indicates a greater number of apoptotic or damaged cells. The results indicated that MP had a protective effect against H_2O_2-induced cell damage.

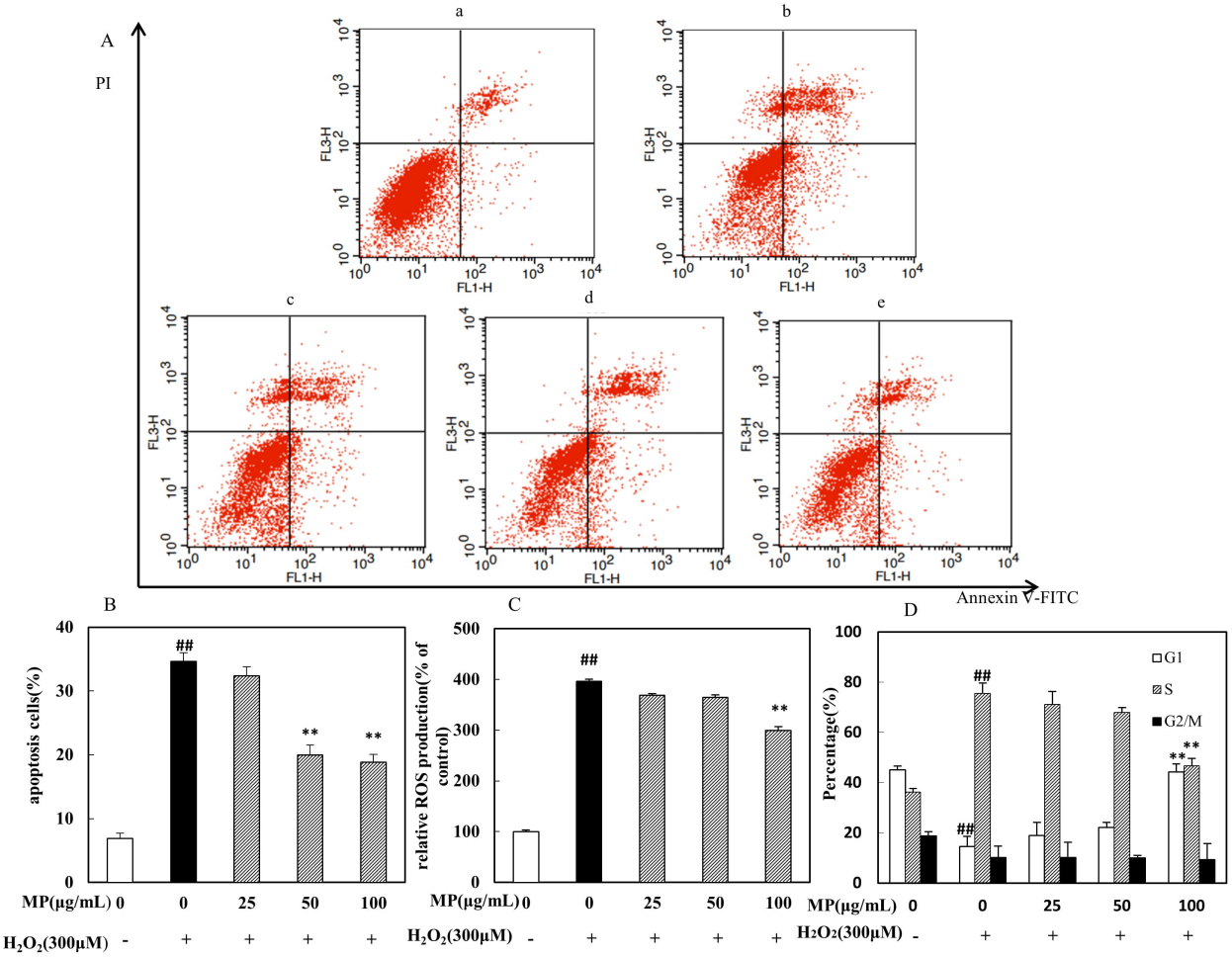

Fig. 4. Effects of MP on SH-SY5Y cells under H_2O_2-induced oxidative stress, as determined by flow cytometry (n = 3). (A,B) Neuroprotective effects of MP in SH-SY5Y cells. (C) Intracellular ROS levels in SH-SY5Y cells. (D) Cell cycle arrest in SH-SY5Y cells. All data are presented as the means ± SDs from three independent experiments performed in triplicate. $^{\#\#}p < 0.01$ versus the control and $^{**}p < 0.01$ versus the H_2O_2 group. Note: In Fig. 4A, (a) control group, (b) H_2O_2 group, (c) H_2O_2 + MP (25 μg/mL) group, (d) H_2O_2 + MP (50 μg/mL) group, and (e) H_2O_2 + MP (100 μg/mL) group.

Increases in the levels of intracellular free radicals or suppression of intracellular antioxidant defense causes oxidative stress [7]. This study found that pretreatment of SH-SY5Y cells with MP significantly reduced the apoptosis rate. This result was consistent with inhibition of the activated fragments of cleaved caspase 3 when cells were treated with MP. The expression of cleaved caspase 3 is low in normal cells, but it is significantly increased in tissue injury models. Intracellular ROS, mainly O_2^-, hydroxyl free radicals (OH) and H_2O_2, are highly active molecules whose content can directly reflect the degree of oxidative stress in cells. MP blocked (attenuated) the production of (and/or scavenged) ROS, which indicates that MP has a certain ability to scavenge free radicals and exert an antioxidant effect; these effects may be related to its neuroprotective effect. MP can also alleviate cell cycle arrest caused by H_2O_2. The cell cycle refers to the entire process of cell proliferation. Protein synthesis occurs in each phase of the cell cycle, while DNA synthesis occurs in the S phase, and RNA synthesis occurs in the G1, S, and G2 phases. When cells are damaged by ROS, they repair DNA damage by inducing cell cycle arrest in the S phase. The H_2O_2-treated cells showed significantly more cell cycle progression than the untreated cells, which were arrested in the S phase. An increase in the proportion of cells in the S phase has been reported to be an indicator of H_2O_2-induced oxidation of cellular targets [40], which is in accordance with the altered cellular redox status detected in exposed cultured cells. Progression to the S phase may also be an adaptive response to oxidative stress. The cell cycle arrest in the current study was significantly attenuated by pretreatment with MP. Cell cycle arrest may be associated with apoptosis, and H_2O_2 has been reported to activate caspase 3 [41]. As shown in Fig. 5, MP significantly suppressed the activity of caspase 3. In addition, P53 protein expression was increased in H_2O_2-treated cells, but MP significantly suppressed P53 expression.

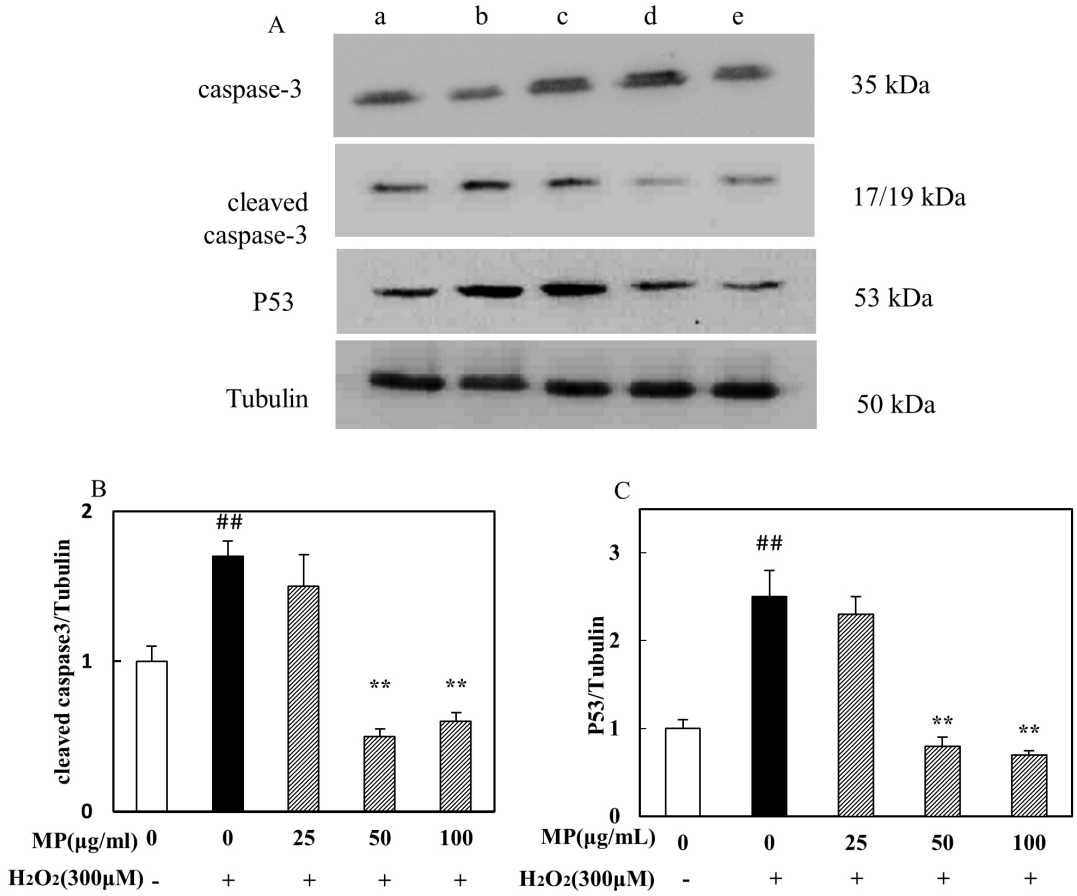

Fig. 5. Effects of MP on cleaved caspase 3 and P53 protein expression in H_2O_2-treated SH-SY5Y cells, as assessed by western blot analysis (n = 3). (A) The expression level of caspase-3, Cleaved caspase-3, P53. (B) The relative expression of cleaved caspase3. (C) The relative expression of P53. All data are presented as the means ± SDs from three independent experiments performed in triplicate. $^{\#\#}p < 0.01$ versus the control; $^{*}p < 0.05$, $^{**}p < 0.01$ versus the H_2O_2 group. Note: In Fig. 5A, (a) control group, (b) H_2O_2 group, (c) H_2O_2 + MP (25 μg/mL) group, (d) H_2O_2 + MP (50 μg/mL) group, and (e) H_2O_2 + MP (100 μg/mL) group.

Clarifying the underlying mechanism of nerve cell damage caused by oxidative stress and elucidating the protective effect of MP on nerve cells will provide an improved theoretical basis for research and further development of the MP mechanism. In this study, we evaluated the antioxidant activity of MP *in vivo* and *in vitro*. In summary, MP alleviated brain tissue injury, as in MP-treated mice, the structure of the hippocampus was relatively normal, the nuclei were round and large, the structural integrity of membranes was retained, GSH-Px activity was increased, and MDA levels were reduced. The results also showed that MP was able to block the production of ROS and ameliorate H_2O_2-induced apoptosis in SH-SY5Y cells. The protective effects of MP were attributable to the modulation of endogenous antioxidant enzymes and ROS scavenging as well as to the modulation of endogenous apoptosis-related protein expression. We have elucidated the underlying cellular mechanisms associated with the protective effects of MP against cellular damage, which are as follows: (1) increases in the activity of antioxidant enzymes, (2) blockade of ROS production, (3) attenuation of cell cycle arrest, and (4) blockade of P53 and cleaved caspase 3 protein expression.

5. Conclusions

MP have protective effects on neuronal oxidative damage models in vivo and in vitro, increased GSH-Px activity, reduced MDA levels, and attenuated the cell damage induced by H_2O_2. Furthermore, MP protected neuronal cells from oxidative stress through a mechanism including a decrease in LDH leakage and reversal of H_2O_2-induced cell morphological damage. MP treatment alleviated the H_2O_2-induced increases in ROS levels, inhibited apoptosis, relieved cell cycle arrest, and downregulated cleaved caspase 3 and P53 protein expression. MP is a novel antioxidant with neuroprotective effects.

Abbreviations

Maca, *Lepidium meyenii* Walp.; MDA, malondialdehyde; LDH, lactate dehydrogenase; ROS, reactive oxygen species; DMSO, dimethyl sulfoxide.

Author contributions

YZhou and LZ—Experimental plan design, manuscript writing, participation in experimental practical work, statistical analysis of data. HL and WX—Preparation and quantification of MP extract. JL—Animal experiment practice work. YZhang—Practical operation of cell experiments. YL and CW—Review of the experimental plan and key revisions.

Ethics approval and consent to participate

The Animal Ethics Committee of Changsha Medical University approved the animal experiments in this study (approval number: 2019042).

Acknowledgment

Not applicable.

Funding

The work was supported by the Natural Science Foundation of Hunan Province (2019JJ50694, 2020JJ5924, 2020JJ3060), the Administration of Traditional Chinese Medicine of Hunan Province (2021075, 202098), the Hunan Provincial Education Commission Foundation (17A026, 18A497, 19C0194, 20C0198), the National Natural Science Foundation of China (81902308), the Provincial Clinical Medical Technology Innovation Project of Hunan (2020SK53710, 2020SK53709), and the Funding by young backbone teachers of Hunan province training program foundation of Changsha Medical University (Hunan Education Bureau Notice 2021 No.29 -26).

Conflict of interest

The authors declare no conflict of interest.

References

[1] Nuñez D, Olavegoya P, Gonzales GF, Gonzales-Castañeda C. Red Maca (Lepidium meyenii), a Plant from the Peruvian Highlands, Promotes Skin Wound Healing at Sea Level and at High Altitude in Adult Male Mice. High Altitude Medicine & Biology. 2017; 18: 372–383.

[2] Pino-Figueroa A, Nguyen D, Maher TJ. Neuroprotective effects of Lepidium meyenii (Maca). Annals of the New York Academy of Sciences. 2010; 1199: 77–85.

[3] Guo SS, Gao XF, Gu YR, Wan ZX, Lu AM, Qin ZH, *et al*. Preservation of Cognitive Function byLepidium meyenii(Maca) is Associated with Improvement of Mitochondrial Activity and Upregulation of Autophagy-Related Proteins in Middle-Aged Mouse Cortex. Evidence-Based Complementary and Alternative Medicine. 2016; 2016: 4394261.

[4] Uchiyama F, Jikyo T, Takeda R, Ogata M. Lepidium meyenii (Maca) enhances the serum levels of luteinising hormone in female rats. Journal of Ethnopharmacology. 2014; 151: 897–902.

[5] Zhong WQ, Liu N, Xie YG, Zhao YM, Song X, Zhong WM. Antioxidant and anti-aging activities of mycelial polysaccharides from Lepista sordida. International Journal of Biological Macromolecules. 2013; 60: 355–359.

[6] Zhu YL, Yu XF, Ge Q, Li J, Wang DJ, Wei Y, *et al*. Antioxidant and anti-aging activities of polysaccharides from Cordyceps cicadae. International Journal of Biological Macromolecules. 2020; 157: 394–400.

[7] Wang L, Oh JY, Kim HS, Lee W, Cui Y, Lee HG, *et al*. Protective effect of polysaccharides from Celluclast-assisted extract of Hizikia fusiforme against hydrogen peroxide-induced oxidative stress *in vitro* in Vero cells and *in vivo* in zebrafish. International Journal of Biological Macromolecules. 2018; 112: 483–489.

[8] Lin LZ, Huang JY, Sun-Waterhouse D, Zhao M, Zhao K, Que J. Maca (Lepidium meyenii) as a source of macamides and polysaccharide in combating of oxidative stress and damage in human erythrocytes. International Journal of Food Science & Technology. 2018; 53: 304–312.

[9] Zha ZQ, Wang SY, Chu WH, Lv Y, Kan HJ, Chen QL, *et al*. Isolation, purification, structural characterization and immunostimulatory activity of water-soluble polysaccharides from Lepidium meyenii. Phytochemistry. 2018; 147: 184–193.

[10] Liao CH, Chen BH, Chiang HS, Chen CW, Chen MF, Ke CC, *et al*. Optimizing a male reproductive aging mouse model by D-galactose injection. International Journal of Molecular Sciences. 2016; 17: 98.

[11] Liu F. Effects Induced by Movement Training and Soy Polypeptide Supplement on D-Galactose Rat Model of Skeletal Muscle Aging. Proceedings of the 2nd International Conference on Biomedical Engineering and Bioinformatics. ACM Digital Library. 2018; 8–13.

[12] Qu P, Li LL, Li H, Wu SW. Intervention of extract from maize embryo on the aging of male rat reproductive system. Journal of Toxicology. 2019; 33: 22–26.

[13] Omidi M, Ahangarpour A, Ali Mard S, Khorsandi L. The effects of myricitrin and vitamin E against reproductive changes induced by D-galactose as an aging model in female mice: An experimental study. International Journal of Reproductive BioMedicine. 2019; 17: 789–798.

[14] Zheng LB, Bai D, Yu Z, Zhang HL, Xie C. Protective effect of skipjack tuna oil against D-galactose-induced aging in mice. Journal of Food Science. 2019; 40: 202–206.

[15] Batista MCA, Abreu BVB, Dutra RP, Cunha MS, Amaral FMM, Torres LMB, *et al*. Chemical composition and antioxidant activity of geopropolis produced by Melipona fasciculata (Meliponinae) in flooded fields and cerrado areas of Maranhão State, northeastern Brazil. Acta Amazonica. 2016; 46: 315–322.

[16] Lima MDS, Silani IDSV, Toaldo IM, Corrêa LC, Biasoto ACT, Pereira GE, *et al*. Phenolic compounds, organic acids and antioxidant activity of grape juices produced from new Brazilian varieties planted in the Northeast Region of Brazil. Food Chemistry. 2014; 161: 94–103.

[17] Jin Y, Wang H. Naringenin Inhibit the Hydrogen Peroxide-Induced SH-SY5Y Cells Injury through Nrf2/HO-1 Pathway. International Journal of Molecular Medicine. 2019; 36: 796–805.

[18] Li Y, Qian L, Jing S, Jin W, Jing G. Mitochondrial protective mechanism of simvastatin protects against amyloid peptide-induced injury in SH-SY5Y cells. International Journal of Molecular Medicine. 2018; 41: 2997–3005.

[19] Xu S, Zhang Y, Jiang K. Antioxidant activity *in vitro* and *in vivo* of the polysaccharides from different varieties of Auricularia auricula. Food & Function. 2016; 7: 3868–3879.

[20] Chen G, Kan J. Ultrasound-assisted extraction, characterization, and antioxidant activity *in vitro* and *in vivo* of polysaccharides from Chestnut rose (Rosa roxburghii tratt) fruit. Journal of Food Science and Technology. 2018; 55: 1083–1092.

[21] Wang DH, Fan B, Wang Y, Zhang LJ, Wang FZ. Optimum Extraction, Characterization, and Antioxidant Activities of Polysaccharides from Flowers of Dendrobium devonianum. International Journal of Analytical Chemistry. 2018; 2018: 3013497.

[22] Roby MHH, Abdelaliem YF, Esmail AM, Mohdaly AAA, Ramadan MF. Evaluation of Egyptian honeys and their floral origins: phenolic compounds, antioxidant activities, and antimicrobial characteristics. Environmental Science and Pollution Research International. 2020; 27: 20748–20756.
[23] Chen SS, Cai F, Wang JR, Yang ZX, Gu C, Wang GF, *et al*. Salidroside protects SH-SY5Y from pathogenic α-synuclein by promoting cell autophagy via mediation of mTOR/p70S6K signaling. Molecular Medicine Reports. 2019; 20: 529–538.
[24] Chain F, Iramain MA, Grau A, Catalán CAN, Brandán SA. Evaluation of the structural, electronic, topological and vibrational properties of N-(3,4-dimethoxybenzyl)-hexadecanamide isolated from Maca (Lepidium meyenii) using different spectroscopic techniques. Journal of Molecular Structure. 2017; 1128: 653–664.
[25] Liu MQ, Li JZ, Kong FZ. Purification, Characterization and Immunological Function of a New Polysaccharide-protein Complex (LE) from Cultured Mycelia of Lentinus edodes. Acta Biochimica et Biophysica Sinica. 1999; 31: 46–50.
[26] Shi JP, Wang JH, Zhang J, Li XL, Tian XY, Wang WG, *et al*. Polysaccharide extracted from Potentilla anserina L ameliorate acute hypobaric hypoxia-induced brain impairment in rats. Phytotherapy Research. 2020; 34: 2397–2407.
[27] Guo H, Kuang Z, Zhang J, Zhao X, Pu P, Yan J. The preventive effect of Apocynum venetum polyphenols on D-galactose-induced oxidative stress in mice. Experimental and Therapeutic Medicine. 2020; 19: 557–568.
[28] Fan SH, Zhang ZF, Zheng YL, Lu J, Wu DM, Shan Q, *et al*. Troxerutin protects the mouse kidney from d-galactose-caused injury through anti-inflammation and anti-oxidation. International Immunopharmacology. 2009; 9: 91–96.
[29] Lei M, Hua XD, Xiao M, Ding J, Han QY, Hu G. Impairments of astrocytes are involved in the d-galactose-induced brain aging. Biochemical and Biophysical Research Communications. 2008; 369: 1082–1087.
[30] Nirmaladevi D, Venkataramana M, Chandranayaka S, Ramesha A, Jameel NM, Srinivas C. Neuroprotective Effects of Bikaverin on H_2O_2-Induced Oxidative Stress Mediated Neuronal Damage in SH-SY5Y Cell Line. Cellular and Molecular Neurobiology. 2014; 34: 973–985.
[31] Mu JF, Wang HL, Wang XD, Sun PD. Expression of miR-124 in gastric adenocarcinoma and the effect on proliferation and invasion of gastric adenocarcinoma SCG-7901 cells. Oncology letters. 2019; 17: 3406–3410.
[32] Shao XR, Wei XQ, Song X, Hao LY, Cai XX, Zhang ZR, *et al*. Independent effect of polymeric nanoparticle zeta potential/surface charge, on their cytotoxicity and affinity to cells. Cell Proliferation. 2015; 48: 465–474.
[33] Li HB, Jiang H, Wang CY, Duan CM, Ye Y, Su XP, *et al*. Comparison of two types of alginate microcapsules on stability and biocompatibility *in vitro* and *in vivo*. Biomedical Materials. 2006; 1: 42.
[34] E. Chain FE, Grau A, Martins JC, Catalán C. Macamides from wild 'Maca', Lepidium meyenii Walpers (Brassicaceae). Phytochemistry Letters. 2014; 8: 145–148.
[35] Ding Q, Wu RA, Yin L, Zhang W, He R, Zhang T, *et al*. Antioxidation and memory protection effects of solid-state-fermented rapeseed meal peptides on D-galactose-induced memory impairment in aging-mice. Journal of Food Process Engineering. 2019; 42: e13145.13141–e13145.13110.
[36] Wang Y, Mao F, Wei X. Characterization and antioxidant activities of polysaccharides from leaves, flowers and seeds of green tea. Carbohydrate Polymers. 2012; 88: 146–153.
[37] Zhong RZ, Xiao WJ, Zhou DW, Tan CY, Tan ZL, Han XF, *et al*. Effect of tea catechins on regulation of cell proliferation and antioxidant enzyme expression in H_2O_2-induced primary hepatocytes of goat *in vitro*. Journal of Animal Physiology and Animal Nutrition. 2013; 97: 475–484.
[38] Satoh T, Sakai N, Enokido Y, Uchiyama Y, Hatanaka H. Free Radical-Independent Protection by Nerve Growth Factor and Bcl-2 of PC12 Cells from Hydrogen Peroxide-Triggered Apoptosis. Journal of Biochemistry. 1996; 120: 540–546.
[39] Yi Z, Jiang H, Xue Y, Liu Y, Li Z, Mu Z, *et al*. Effects of milk with inulin and vitamin D_3 on bone health and gastrointestine symptoms in lactose intolerance population. Journal of Hygiene Research. 2016; 45: 801–806. (In Chinese)
[40] Hampton MB, Orrenius S. Dual regulation of caspase activity by hydrogen peroxide: implications for apoptosis. FEBS Letters. 1997; 414: 552–556.
[41] Chua SK, Wang BW, Lien LM, Lo HM, Chiu CZ, Shyu KG. Mechanical Stretch Inhibits MicroRNA499 via p53 to Regulate Calcineurin-A Expression in Rat Cardiomyocytes. PLoS ONE. 2016; 11: e0148683.